

A NEAR-FIELD MEASUREMENT MODEL FOR ULTRASONIC REFERENCE STANDARDS

Lester W. Schmerr Jr.

Center for NDE and the Department of Aerospace
Engineering and Engineering Mechanics
Iowa State University, Ames, Iowa 50011

Alexander Sedov

School of Engineering
Lakehead University, Thunder Bay, Ontario
Canada P7B5E1

INTRODUCTION

Recent modelling studies [1], [2] have shown that it is possible to develop simple analytical expressions for the scattering of flat-bottom holes and spheres that can be used for quantitative ultrasonic calibration measurements. In the flat-bottom hole case these models have been tested experimentally, yielding excellent agreement even well into the near-field region of the transducer [3].

Here we will describe how similar modelling concepts can be used to predict the measured pulse-echo response of an arbitrary reference scatterer on the axis of a piston transducer in a fluid. The model makes no apriori assumptions about either the shape or material property of the scatterer and does not require that the scatterer necessarily be in the far-field of the transducer. Thus, the model demonstrates how the far-field measurement model of Thompson and Gray [4] can be extended, for this configuration, to the near-field while still retaining explicit analytical expressions that can be easily calculated.

THE MODEL

The scattering model developed here is based on four main ideas: (1) the use of a superposition of plane waves to produce the incident bounded sound beam from a piston source, (2) the use of the T-matrix form of the scattered waves to express the response of the scatterer to the finite beam in terms of spherical waves, (3) the transformation from spherical wave to cylindrical wave coordinates so that the scattered waves can be suitably averaged over the receiving transducer surface, and finally (4) the use of high frequency asymptotics and far-field scattering amplitude expressions to reduce the model to the sum of simple analytical expressions. Below we outline briefly each part of the resulting model.

Incident and scattered waves

Consider an arbitrary flaw immersed in a fluid medium and subjected to an incident plane wave propagating in a general direction, \mathbf{e}_i , as shown in Fig. 1. It is well known that the incident plane wave pressure, p^{inc} , can be expressed in terms of spherical (standing) waves as [5]:

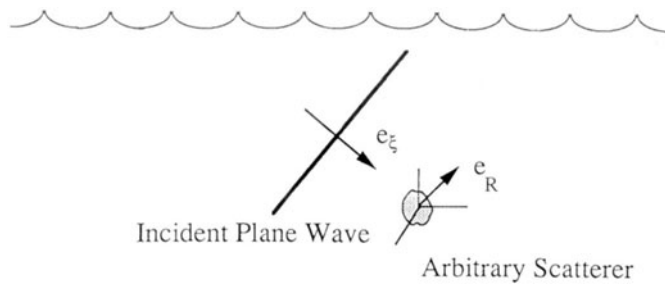


Fig. 1. Plane wave incident on an arbitrary scatterer in a fluid.

$$p^{inc} = \exp(ik\underline{e}_\xi \cdot \underline{x}) = \sum_{m=0}^{\infty} \sum_{l=-m}^m a_{ml} j_m^{(1)}(kR) Y_{ml}(\underline{e}_R) \quad (1)$$

where k is the wavenumber and

$$a_{ml} = i^m (-1)^l \left[\frac{4\pi(2m+1)(m-1)!}{(m+1)!} \right]^{1/2} P_m^l(\cos\theta_\xi) \cdot \exp(-il\phi_\xi) \quad (2)$$

with $\underline{x} = R\underline{e}_R$ in spherical coordinates and where (θ_ξ, ϕ_ξ) are the spherical coordinates of the incident wave direction \underline{e}_ξ (Fig. 1). Similarly, the pressure in the waves scattered from the flaw, can be represented in spherical wave form as

$$p^{scatt} = \sum_{p=0}^{\infty} \sum_{q=-p}^p \sum_{m=0}^{\infty} \sum_{l=-m}^m T_{pqml} a_{ml} h_p^{(1)}(kR) Y_{qp}(\underline{e}_R) \quad (3)$$

where the T-matrix is determined explicitly from the flaw geometry [6].

Bounded beam solutions

Uberall [7] has shown how the incident bounded beam pressure, p_{beam}^{inc} , generated from a circular piston transducer radiating with a uniform velocity v_0 (Fig. 2) can be generated through a superposition of the incident waves, p^{inc} . Explicitly, this superposition is

$$p_{beam}^{inc} = 1/(2\pi)^2 \int_0^{2\pi} \int_0^\infty p^{inc} \Phi(\xi) \exp(iz_0 \sqrt{k^2 - \xi^2}) \xi d\xi d\phi_\xi \quad (4)$$

where

$$\Phi(\xi) = (2\pi\rho v_0 a / \sqrt{k^2 - \xi^2}) J_1(\xi a) / \xi a \quad (5)$$

and ρ is the density of the fluid. From eqs. (3), (4), (5) this bounded incident beam then produces a scattered pressure, p_{beam}^{scatt} , given by

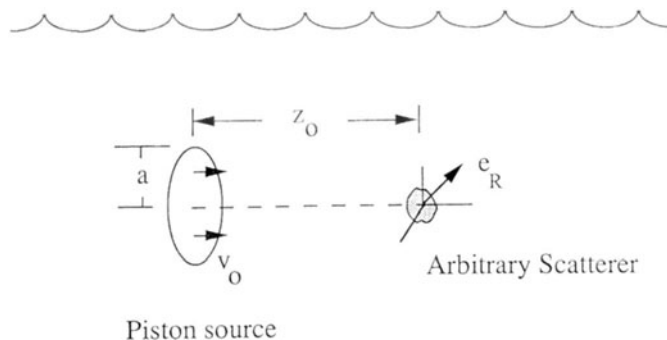


Fig. 2. Bounded beam (piston source) incident on an arbitrary scatterer in a fluid.

$$p_{\text{beam}}^{\text{scatt}} = \sum_{p=0}^{\infty} \sum_{q=-p}^p \sum_{m=0}^{\infty} \sum_{l=-m}^m T_{pqml} I_m^1(a_{ml}) h_p^{(1)}(kR) Y_{qp}(\underline{e}_R) \quad (6)$$

where

$$I_m^1(a_{ml}) = \delta_{l0} (-1)^l (i)^m \left[\frac{(2m+1)(m-1)!}{\pi(m+1)!} \right]^{1/2} \cdot \int_0^{\infty} \Phi(\xi) P_m^l(\cos \theta_{\xi}) \exp(i z_o \sqrt{k^2 - \xi^2}) \xi d\xi \quad (7)$$

and δ_{l0} is the kronecker delta.

The reception process

It is the scattered wavefield in eq. (6) that impinges on the piston transducer during the reception process. Here, we will assume that the voltage received by the transducer is proportional to the average received normal velocity, $\langle v_z \rangle$, where the velocity is given by

$$v_z = (1/i\omega\rho) \partial p / \partial z$$

The corresponding average velocity is

$$\langle v_z \rangle = 1/\pi a^2 \int_0^a v_z 2\pi r dr \quad (8)$$

where r is the radial location of an arbitrary point on the transducer surface. However, because the scattered waves in eq. (6) are in terms of spherical waves, the calculation of $\langle v_z \rangle$ is not directly possible. Thus, we first transform the spherical waves in eq. (6) to cylindrical waves via [5].

$$h_p^{(1)}(kR) P_p^q(\cos \theta) = i^{q+p}/k \int_0^{\infty} J_q(\xi r) P_p^q(\sigma/k) \cdot \exp(i|z|\sigma) \xi d\xi / \sigma \quad (9)$$

where

$$\sigma = \operatorname{sgn} k \sqrt{k^2 - \xi^2} \quad (10)$$

Then the calculation of v_z and its average, $\langle v_z \rangle$, can be carried out explicitly. We find

$$\langle v_z \rangle = \sum_{p=0}^{\infty} \sum_{m=0}^{\infty} T_{p0m0} I_m^1 I_p^2 \quad (11)$$

with

$$I_m^1 = (\rho \omega v_0 a) i^m \sqrt{4\pi(2m+1)} \int_0^\infty J_1(\xi a) P_m(\sigma/k) \cdot \exp(i\sigma z_0) \xi d\xi / \sigma \quad (12)$$

$$I_p^2 = -2i^p / (\rho \omega k a) \sqrt{(2p+1)/4\pi} \int_0^\infty J_1(\xi a) P_p(\sigma/k) \cdot \exp(i\sigma z_0) d\xi \quad (13)$$

Equation (11) is an exact result. It gives the average velocity received by a transducer from an arbitrary scatterer on the axis of that transducer, assuming the transducer acts as a uniform piston source.

Unfortunately, Eq. (11) is not in a form suitable for practical evaluation because it involves the calculation of two semi-infinite integrals and two semi-infinite summations, as well as requiring the calculation of an infinite set of T-matrix values.

High frequency (stationary phase) approximation

To turn eq. (11) into a more useful form, we first note that both the integrals I_m^1 and I_p^2 are of a form that we have encountered before in our flat-bottom hole and sphere models and can, as we have shown previously, be evaluated explicitly by the method of stationary phase for $ka \gg 1$ [1], [2]. Since most ultrasonic transducers operate at wavelengths considerably smaller than the transducer radius, this high frequency approximation is not likely to be violated in most testing situations. Following the procedures outlined in [1], therefore, we obtain explicitly

$$I_m^1 = (\rho v_0 c) i^m \sqrt{4\pi(2m+1)} [\exp(ikz_0) - P_m(\cos \alpha) \cdot \exp(ik\sqrt{a^2 + z^2})] \quad (14)$$

$$I_p^2 = -2i^p c / (\rho \omega^2 a^2) \sqrt{(2p+1)/4\pi} [\exp(ikz_0) - \cos \alpha P_p(\cos \alpha) \exp(ik\sqrt{a^2 + z^2})] \quad (15)$$

where the angle α is from the edge of the transducer to the origin of the coordinates as shown in Fig. 2.

It is interesting that when these expressions are placed back into eq. (11), the resulting expression contains four terms, each of which can be given a physical interpretation in terms of direct and edge wave "ray-like" contributions just as in our previous flat-bottom hole and sphere models [2]. These terms can be made even more explicit by noting that the far-field scattering amplitude of an arbitrary scatterer due to an incident plane wave can be written, in T-matrix form, as

$$f(\theta_i, \phi_i, \theta_r, \phi_r) = 1/k \sum_{p=0}^{\infty} \sum_{q=-p}^p \sum_{m=0}^{\infty} \sum_{l=-m}^m T_{pqml} a_{ml}(-i)^{p+1} Y_{qp}(e_R) \quad (16)$$

where (θ_i, ϕ_i) and (θ_r, ϕ_r) are the spherical coordinates of the incident and scattered wave directions, respectively. Then it follows that

$$f(0, \cdot; \pi, \cdot) = 1/ik \sum_{p=0}^{\infty} \sum_{m=0}^{\infty} T_{p0m0} \sqrt{(2m+1)(2p+1)} i^p i^m \quad (17a)$$

$$\begin{aligned} \langle f(0, \cdot; \pi - \alpha, \phi_r) \rangle_{\phi_r} &= 1/ik \sum_{p=0}^{\infty} \sum_{m=0}^{\infty} T_{p0m0} \sqrt{(2m+1)(2p+1)} \\ &\cdot P_p(\cos \alpha) i^p i^m \end{aligned} \quad (17b)$$

$$\begin{aligned} \langle f(\alpha, \phi_i; \pi, \cdot) \rangle_{\phi_i} &= 1/ik \sum_{p=0}^{\infty} \sum_{m=0}^{\infty} T_{p0m0} \sqrt{(2m+1)(2p+1)} \\ &\cdot P_m(\cos \alpha) i^p i^m \end{aligned} \quad (17c)$$

$$\begin{aligned} \ll f(\alpha, \phi_i; \pi - \alpha, \phi_r) \gg_{\phi_i, \phi_r} &= 1/ik \sum_{p=0}^{\infty} \sum_{m=0}^{\infty} T_{p0m0} \sqrt{(2m+1)(2p+1)} P_m(\cos \alpha) \\ &\cdot P_p(\cos \alpha) i^p i^m \end{aligned} \quad (17d)$$

where the brackets indicate an average over either the incident or scattered ϕ -angle, i.e.

$$\langle f \rangle_{\phi_m} = 1/2\pi \int_{\phi_m=0}^{2\pi} f d\phi_m \quad (m=i, r)$$

and an argument of f is omitted if it is independent of that argument.

An examination of eq. (11) shows that it contains each of the four terms in eqs. (17a-d) so that we have, finally

$$\begin{aligned} \langle v_z \rangle &= -2v_0/a^2 k^2 \{ \exp(2ikz_0) ik f(0, \cdot; \pi, \cdot) \\ &- \cos \alpha \exp[ik(z_0 + \sqrt{a^2 + z_0^2})] ik \langle f(0, \cdot; \pi - \alpha, \phi_r) \rangle_{\phi_r} \\ &- \exp[ik(z_0 + \sqrt{a^2 + z_0^2})] ik \langle f(\alpha, \phi_i; \pi, \cdot) \rangle_{\phi_i} \\ &+ \cos \alpha \exp[2ik\sqrt{a^2 + z_0^2}] ik \ll f(\alpha, \phi_i; \pi - \alpha, \phi_r) \gg_{\phi_i, \phi_r} \} \end{aligned} \quad (18)$$

Equation (18) is our general near-field measurement model result. It shows that for $ka \gg 1$ the average velocity received from an arbitrary scatterer can be written in an explicit form in terms of four (suitably averaged) plane wave far-field scattering amplitudes. Since computing plane wave scattering amplitudes can be done by a variety of methods, including separation of variables (for a sphere), numerical methods (boundary elements, T-matrix methods, etc.) and approximate methods (Born, Kirchhoff, low frequency approximations, etc.), eq. (18) gives a general "template" to place these calculations into and obtain the measured response in a pulse-echo reference scattering setup. Below, we illustrate this procedure for the cases of cylindrical and spherical scatterers.

Special cases

Far-field Limit

When the angle α is small, the far-field scattering amplitudes appearing in eq. (18) are all nearly independent of ϕ and $\cos \alpha \approx 1$ so that we obtain approximately

$$\begin{aligned} \langle v_z \rangle &= 2v_o / ika^2 [\exp(ikz_o) - \exp(ik\sqrt{a^2 + z_o^2})]^2 \\ &\cdot f(0, \cdot; \pi, \cdot) \end{aligned} \quad (19)$$

which is identical in form to that obtained using the far-field measurement model of Thompson and Gray[4]. In the far-field limit we see that the transducer diffracted wavefields and scatterer responses decouple and the measured response is proportional to the backscattered far-field scattering amplitude of the scatterer. In the near-field, eq. (18) shows that the transducer and scatterer responses are inherently intermixed.

Axisymmetric Scatterer

Many reference scatterers that are used in calibration setups, such as the sphere, are axisymmetric in geometry. In this case eq. (18) simplifies even further and we obtain

$$\begin{aligned} \langle v_z \rangle &= -2v_o / a^2 k^2 \{ \exp(2ikz_o) i k f(0, \cdot; \pi, \cdot) \\ &- \cos \alpha \exp[ik(z_o + \sqrt{a^2 + z_o^2})] i k f(0, \cdot; \pi - \alpha, \cdot) \\ &- \exp[ik(z_o + \sqrt{a^2 + z_o^2})] i k f(\alpha, \cdot; \pi, \cdot) \\ &+ \cos \alpha \exp[2ik\sqrt{a^2 + z_o^2}] i k \langle f(\alpha, \cdot; \pi - \alpha, \phi_r) \rangle_{\phi_r} \} \end{aligned} \quad (20)$$

where all the averages are gone except for the last "edge to edge" term [1]. Two special cases that are of this type are the cylindrical scatterer (Fig. 3a) and the sphere (Fig. 3b). In the Kirchhoff approximation we find, for a rigid cylinder

$$\begin{aligned} f(0, \cdot; \pi) &= -ikb^2/2 \\ f(0, \cdot; \pi - \alpha, \cdot) &= -ikb J_1(kb \sin \alpha) / k \sin \alpha \\ f(\alpha, \cdot; \pi, \cdot) &= -ikb \cos \alpha J_1(kb \sin \alpha) / k \sin \alpha \end{aligned}$$

$$\langle f(\alpha, \cdot; \pi - \alpha, \phi_r) \rangle_{\phi_r} = -ikb^2 \cos \alpha [J_0^2(kb \sin \alpha) + J_1^2(kb \sin \alpha)]/2$$

which agree with the analogous results we obtained earlier in our flat-bottom hole model. Similarly, for a rigid spherical scatterer in the Kirchhoff approximation, we obtain explicitly

$$f(0, \cdot; \pi, \cdot) = b \exp(-2ikb)/2$$

$$f(0, \cdot; \pi - \alpha, \cdot) = b \exp(-2ikb \cos \alpha/2)/2$$

$$f(\alpha, \cdot; \pi, \cdot) = b \exp(-2ikb \cos \alpha/2)/2$$

$$\langle f(\alpha, \cdot; \pi - \alpha, \phi_r) \rangle_{\phi_r} = b/4\pi \int_0^{2\pi} \exp[-ikb \sqrt{2 + 2\cos^2 \alpha + 2\sin^2 \alpha \cos \phi_r}]$$

$$\cdot d\phi_r$$

$$\approx b/2 \exp[-ikb \sqrt{2 + 2\cos \alpha}] J_0(kb \sin^2 \alpha / \sqrt{2 + 2\cos \alpha})$$

for small α

Again, these reduce to our previous results for the sphere. Thus, we see our earlier model results [1] [2] are contained as special cases of our general expression, eq. (18).

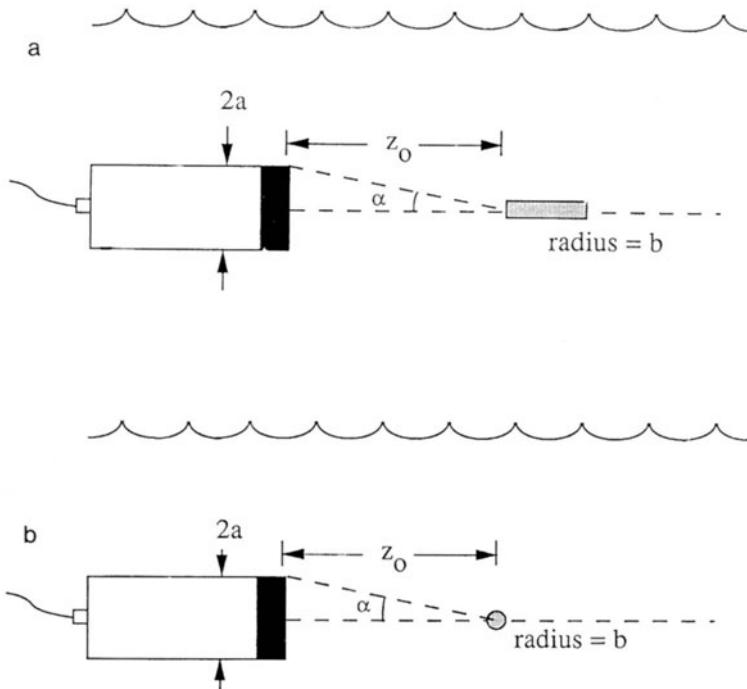


Fig. 3 3a. Scattering geometry for a rigid cylindrical scatterer.
3b. Scattering geometry for a rigid spherical scatterer.

CONCLUSIONS

We have shown how a near-field measurement model can be developed to predict the pulse echo response of an arbitrary scatterer on the axis of a piston transducer in a fluid. The model generalizes our earlier flat-bottom hole and sphere scattering models and reduces to the far-field measurement model of Thompson and Gray when the scatterer is in the transducer far-field. Since our model is not restricted to far-field conditions, it effectively extends the Thompson-Gray model into the near-field for this problem and can be used to estimate model errors present when far-field conditions are not satisfied exactly. The generality and simplicity of the model should allow it to serve as an important ingredient in a variety of quantitative ultrasonic calibration and standards procedures.

ACKNOWLEDGEMENTS

A. Sedov was supported in this work by the National Sciences and Engineering Research Council of Canada. This work was also supported, for L. W. Schmerr, by the Center for NDE, Iowa State University.

REFERENCES

1. Schmerr, L. W. and A. Sedov, "The Flat-Bottom Hole: An Ultrasonic Scattering Model," Res. Nondestr. Eval., 1, pp. 181-196, 1989.
2. Sedov, A., Schmerr, L. W. and S. J. Song, "Ultrasonic Scattering Models for Standards: Flat-Bottom Holes and Spherical Reflectors," Review of Progress in Quantitative NDE, D. O. Thompson and D. E. Chimenti, Eds., Vol. 10A, pp. 59-65, 1991.
3. Song, S. J., Schmerr, L. W., and A. Sedov, "DGS Diagrams and Frequency Response Curves for a Flat-Bottom Hole: A Model-based Approach," Res. Nondestr. Eval (to appear), 1991.
4. Thompson, R. B. and T. A. Gray, "A Model Relating Ultrasonic Scattering Measurements Through Liquid-Solid Interfaces to Unbounded Medium Scattering Amplitudes," J. Acoust. Soc. Am., 74, pp. 1279-1290, 1983.
5. Ben-Menahem, A. and S. J. Singh, Seismic Waves and Sources, Springer-Verlag, New York, 1981.
6. Ishimaru, A., Electromagnetic Wave Propagation, Radiation, and Scattering, Prentice Hall, Englewood Cliffs, N.J., 1991.
7. Gaunard, G. C. and H. Uberall, "Acoustics of Finite Beams," J. Acoust. Soc. Am., 63, pp. 5-16, 1978.